Molding light flow from photonic band gap circuits to microstructured fibers

James Bauer[a)] and Sajeev John

Department of Physics, University of Toronto, 60 St. George Street, Toronto, Ontario M5S 1A7, Canada

The authors demonstrate nearly lossless, broadband coupling of light between photonic band gap (PBG) circuits and photonic crystal fibers (PCFs) using two-dimensional design paradigms. A hollow-core PBG fiber yields a coupling efficiency of better than 94% over a bandwidth of 25% of the center frequency, with peak transmittance exceeding 98%. A small-mode-area PCF consisting of a subwavelength solid core with nonadiabatic taper, combined with a PBG beam collimator at the air-waveguide exit port, yields over 98% coupling efficiency over a bandwidth of 135 nm centered at a wavelength of 1.5 μm. © *2007 American Institute of Physics*. [DOI: 10.1063/1.2752732]

Since the introduction of photonic band gap (PBG) materials[1,2] a central challenge to their practical application in optical communications is the design of lossless, broadband interconnects to optical fibers. In contrast to light guidance by total internal reflection (index guiding), PBG-based microcircuits can guide light in air-core waveguides by interference (localization) effects.[3] One platform for implementing broadband three-dimensional (3D) integrated optics is in PBG heterostructures,[4–7] which posses a full 3D PBG and the intercalated two-dimensional (2D) microchip layer allows embedding of previous 2D designs in a three dimensional setting without out-of-plane scattering loss. In this letter, we present two-dimensional paradigms for beam collimation and small "footprint," low-loss, broadband coupling between microstructured fibers and PBG microchips. These concepts suggest that near perfect transfer of optical information from PBG circuits to fiber-optic networks may, in principle, be realized.

Previous attempts at coupling light into photonic crystal (PC) waveguides from external sources can be classified into various categories. The first is adiabatic coupling, where the waveguide is slowly changed over tens to hundreds of PC unit cells.[8,9] A second approach relies on transferring light from high-index PC waveguides to high-index "slab" waveguides,[10,11] that then require a large footprint to adiabatically connect with optical fibers. A third approach considers coupling into low-index PBG waveguides using various PC "horns"[12] with sharp tapers. The best reported coupling efficiency is 93.5%, without mention of coupling bandwidth.[13] A fourth strategy involves coupling into PC "membrane" waveguides using tapered optical fibers.[14,15] This yields up to 95% coupling efficiency but only over a bandwidth of about 1%.[16] In contrast to earlier approaches, we exploit the design flexibility of microstructured optical fibers[17–23] to simultaneously obtain "small-footprint," broadband, and nearly lossless coupling to PBG circuits.

The dimensional reduction of a 2D-3D PBG heterostructure air-waveguide exit port is the corresponding surface termination of a 2D square lattice of dielectric rods embedded in air [see Figs. 1(a) and 1(b)]. A square lattice of dielectric rods (ϵ_{rod}=11.9) of radius r=0.15a (where a is the lattice constant of the PC) embedded in air has a 2D PBG between

(a/λ)=0.330 and (a/λ)=0.475 (where λ is the free-space wavelength) for the modes with electric field polarized along the rods. A single-mode waveguide that spans the frequency range of the band gap is created by removing one row of rods.

Light exiting an aperture smaller than the free-space wavelength (such as the PC air-waveguide exit port) experiences severe diffraction.[24] We solve this problem by designing a π phase-shifted wave field from a secondary source placed near the waveguide mouth, that is driven by light from the waveguide. This cancels diffraction at certain angles through destructive interference with the wave field from the primary source (the waveguide itself). Figure 2 depicts a modified waveguide exit port in which two dielectric rods are removed and the next two dielectric rods have been replaced by larger rods of radius r_{exit}=0.275a. Below resonance at $a/\lambda \approx 0.37$, the secondary sources emit in phase
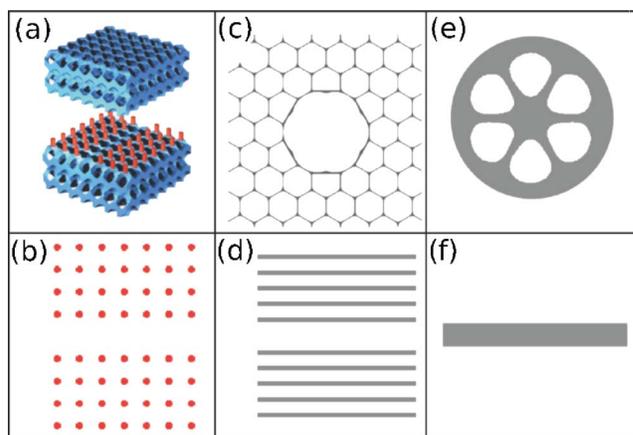
FIG. 1. (Color online) (a) Depicted is an air waveguide in a 2D-3D PBG heterostructure, consisting of a 2D lattice of square rods sandwiched between two 3D PBG materials above and below. A single-mode waveguide is created by removing a row of rods in the 2D layer. (b) The 2D model of the waveguide from (a) is a 2D lattice of dielectric rods with a missing row. (c) Shows a cross section of a hollow core PBG fiber. The large central (air) defect supports a guided mode (sometimes multiple modes) that is radially contained by the PBG effect. This structure is invariant along the fiber axis. (d) depicts our 2D model of the fiber in (c). This fiber Bragg waveguide, like its 3D counterpart, contains light primarily in the air defect, confined through wave interference rather than total internal reflection. (e) shows a schematic of a small-mode-area fiber where a dielectric island is supported by thin dielectric veins. This fiber is modeled in 2D as a dielectric slab (f).

---

a)Electronic mail: jbauer@physics.utoronto.ca

90, 261111-1
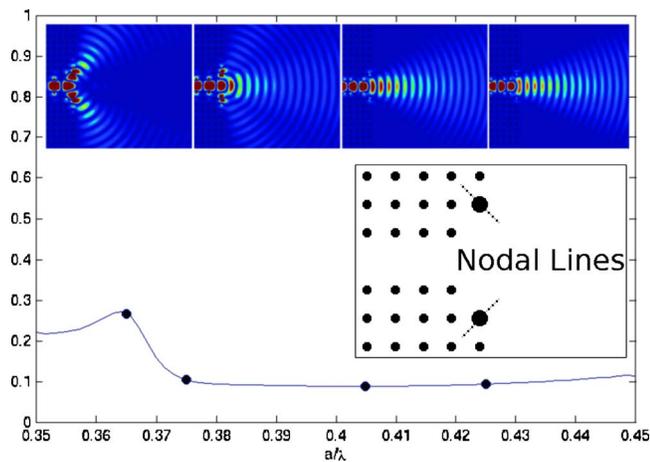
FIG. 2. (Color online) PBG exit-port beam collimator. The first nearest neighbor rods at the exit have been removed and the second nearest neighbor rods have radius $r_{exit}=0.275a$. The blue curve shows the reflectance back into the PC waveguide. Snapshots of the electric field intensity at frequencies (from left to right) $(a/\lambda)=(0.365, 0.375, 0.405, \text{and } 0.425)$ are also shown. The beam collimation is achieved over a broad range of frequencies above the resonance $a/\lambda \approx 0.37$. This arises from destructive interference between the standard diffraction pattern from the waveguide exit port and the π shifted light from the resonators in the off-axis direction.

FIG. 3. (Color online) Transmittance (upper curve) and reflectance (lower curve) for light coupling from the PBG air waveguide to the hollow core PBG fiber (see inset). The PBG air waveguide parameters are $\epsilon_{rod}=11.9$, $\epsilon_{background}=1.0$, and $r=0.15a$, where a is the PC lattice constant. The hollow core fiber has $D=1.6A$, $d_1=0.3A$, $d_2=0.7A$, with refractive indices $n_1=1.8$, $n_2=1.0$, where A is the fiber cladding lattice constant. The two lattice constants are related by $A/a=1.3$.

with the direct waveguide diffraction pattern at angles nearly perpendicular to the indicated nodal lines. This leads to a marked increase in off-axis diffraction (for example, at $a/\lambda =0.365$). However, above resonance the π phase shift in the secondary emission cancels almost all unwanted diffraction, leading to a broad band (17.5%) of beam collimation. The resulting band is much broader than the narrow working range of previous designs based on lossy surface modes.[25,26] Our physically motivated design provides insight beyond that available from purely computational search algorithms.[27]

We now combine various PBG exit port designs with various microstructured optical fibers [see Figs. 1(c)–1(f)] and show that large bandwidth near perfect transmission is possible. The two-dimensional analog of a hollow core PBG fiber is a low-index (air) defect core sandwiched above and below by one-dimensional Bragg stacks [see Figs. 1(c) and 1(d)]. Waveguide modes occur because the enlarged core (defect) confines a fundamental even mode within the one-dimensional band gap of the surrounding cladding. The fiber (Bragg waveguide) parameter space spans a defect width D between $1.2A$ and $2.1A$ (where A is the Bragg cladding lattice constant), a variation in n_1 between 1.5 and 1.8 (with $n_2=1.0$), and a variation A/a from 1.2 to 2.0. We use the finite-difference time-domain method with perfectly matched layer boundary conditions[28] to calculate the reflectance and transmittance spectra for the family of different 2D fiber models. The 2D hollow core fiber is placed immediately adjacent to the last row of rods of the PC.

Figure 3 shows the reflectance and transmittance spectra for the structure with the highest transmittance within the parameter space. The reflectance is below 2% and the transmittance is better than 94% from $(a/\lambda)=0.35$ to $(a/\lambda)=0.45$. The back-reflection into the PC waveguide when coupled to the fiber is lower than if the PC waveguide simply diffracts or beams light to free space. Inclusion of the beam collimator (in Fig. 2) for coupling to this hollow core PBG fiber is redundant and unnecessary.

An alternative to the hollow core PBG fiber is the "small-mode-area" PC fiber.[29] This fiber has a small silica core ($\approx 1 \ \mu m^2$ cross section) supported by a thin network of silica veins in air. The two-dimensional analog of a small-mode-area solid-core fiber [see Figs. 1(e) and 1(f)] is a dielectric slab surrounded by air (the thin network of silica veins connecting the solid core to the outer cladding is neglected in our 2D model). Here, we choose the refractive index of the core $n_{core}=1.5$ and the immediate surrounding to be $n_{clad}=1.0$. We consider only even modes that have the same polarization as the PC waveguide. The odd modes and TE modes of the fiber do not couple with the even TM PC waveguide mode. We also restrict the slab width w so that only a single, highly concentrated mode is supported in the frequency range of interest.

With unmodified PC air waveguide and butt-coupled small-area ($w=1.5a$) solid-core [photonic crystal fiber slab waveguides as in Fig. 1(f)], we find that the transmittance ranges between 82% and 84.5% for the entire bandwidth. The reflectance varies between 8% and 2%. The remaining fraction of the energy is lost symmetrically on either side of the fiber through diffraction. By incorporating the exit-port collimator of Fig. 2, diffraction can nearly be eliminated, with peak transmittance improving to near 94% over 17% of the center frequency. Nevertheless, we find that for all parameters studied (fiber position and fiber core diameter), a 2%–5% back reflection persists over the frequency range. This problem is solved using a nonadiabatic taper in the solid core.

The best available coupling is obtained by tapering the solid-core fiber and allowing the tapered end to enter the exit-port collimator. Figure 4 shows reflectance and transmittance for the PC air waveguide to tapered fiber interface, including the collimator. The reflectance is now less than 1% between $(a/\lambda)=0.38$ and 0.445, and the collimator nearly eliminates off-normal diffractive losses. Near elimination of diffractive losses combined with eradication of back reflection lead to a transmittance of more than 98% over a bandwidth of 9% of the center frequency. At present-day telecommunication frequencies (1.5 μm), this covers a bandwidth of
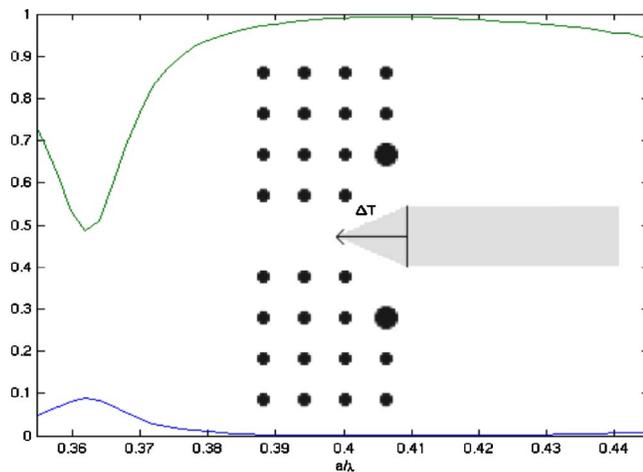
FIG. 4. (Color online) Transmittance (upper curve) and reflectance (lower curve) for light coupling from a PBG air waveguide (with the beam collimator) to a tapered, small-mode-area, solid-core fiber. The PBG parameters are $\epsilon_{rod}=11.9$, $\epsilon_{background}=1.0$, with collimator rod radius $r_{exit}=0.275a$ and bulk rod radius $r=0.15a$, where a is the PC lattice constant. The fiber core parameters are $\epsilon_{slab}=2.25$, $w=1.5a$, and $\Delta T=1.75a$. Here, over 98% coupling efficiency is achieved over a range of 9% of the optimum wavelength defined by $a/\lambda=0.41$. If this optimum wavelength is chosen to be 1.5 μm, then this near perfect coupling is maintained over a bandwidth of 135 nm.

135 nm. Here, the collimator eliminates off-axis diffractive losses and the taper plays two roles: to reduce back reflectance and to facilitate conversion of the PC waveguide mode to the fiber core mode. Note that the resonant frequency of the beam collimator may be tuned to higher or lower values by tuning the size of the modified exit rods.

In summary, we have shown using a 2D model that by combining beam collimation at the PBG chip exit port with suitably microstructured PBG fibers, large bandwidth, low-loss coupling is possible. These 2D design paradigms suggest that similar high efficiency coupling may be possible in realistic 3D fiber to chip junctions, provided that certain loss conditions are observed.[30] After interfacing with PBG microchips, the specialty PC fibers proposed here may then be adiabatically tapered over centimeter scales to merge into more conventional long-haul optical fibers. This will greatly facilitate the deployment of PBG microchips in optical communications and information processing.

[1] S. John, Phys. Rev. Lett. **58**, 2486 (1987).
[2] E. Yablonovitch, Phys. Rev. Lett. **58**, 2059 (1987).
[3] S. John, Phys. Rev. Lett. **53**, 2169 (1984).
[4] A. Chutinan, S. John, and O. Toader, Phys. Rev. Lett. **90** (2003).
[5] A. Chutinan and S. John, Phys. Rev. E **71** (2005).
[6] A. Chutinan and S. John, Opt. Express **14**, 1266 (2006).
[7] M. Deubel, M. Wegener, S. Linden, G. V. Freymann, and S. John, Opt. Lett. **31**, 805 (2006).
[8] Y. Xu, R. K. Lee, and A. Yariv, Opt. Lett. **25**, 755 (2000).
[9] A. Mekis and J. D. Joannopoulos, J. Lightwave Technol. **19**, 861 (2001).
[10] A. Adibi, Y. Xu, R. K. Lee, A. Yariv, and A. Scherer, Phys. Rev. B **64** (2001).
[11] E. Miyai, M. Okano, M. Mochizuki, and S. Noda, Appl. Phys. Lett. **81**, 3729 (2002).
[12] P. Sanchis, J. Marti, J. Blasco, A. Martinez, and A. Garcia, Opt. Express **10**, 1391 (2002).
[13] J. Jiang, J. Cai, G. P. Nordin, and L. Li, Opt. Lett. **28**, 2381 (2003).
[14] P. E. Barclay, K. Srinivasan, and O. Painter, PECS-IV: International Workshop on Photonic and Electromagnetic Crystal Structures, University of California, Los Angeles (2002), p. 38.
[15] W. Kuang, C. Kim, A. Stapleton, and J. D. O'Brien, Opt. Lett. **27**, 1604 (2002).
[16] P. E. Barclay, K. Srinivasan, and O. Painter, J. Opt. Soc. Am. B **20**, 2274 (2003).
[17] A. Ferrando, E. Silvestre, J. J. Miret, and P. Andres, Opt. Lett. **25**, 790 (2000).
[18] J. C. Knight, J. Arriaga, T. A. Birks, A. Ortigosa-Blanch, W. J. Wadsworth, and P. S. J. Russell, IEEE Photonics Technol. Lett. **12**, 807 (2000).
[19] T. A. Birks, J. C. Knight, and P. S. J. Russell, Opt. Lett. **22**, 961 (1997).
[20] R. F. Cregan, B. J. Mangan, J. C. Knight, T. A. Birks, P. S. J. Russell, P. J. Roberts, and D. C. Allan, Science **285**, 1537 (1999).
[21] J. C. Knight, J. Arriaga, T. A. Birks, A. Ortigosa-Blanch, W. J. Wadsworth, and P. S. J. Russell, IEEE Photonics Technol. Lett. **12**, 807 (2000).
[22] J. Broeng, S. E. Barkou, and A. Bjarklev, Opt. Fiber Commun. **3**, 101 (2000).
[23] D. Moss, Y. Miao, V. Ta'eed, E. Magi, and B. Eggleton, Electron. Lett. **41**, 951 (2005).
[24] J. D. Jackson, *Classical Electrodynamics*, 3rd ed. (Wiley, New York, 1999), p. 492.
[25] P. Kramper, M. Agio, C. M. Soukoulis, A. Birner, F. Muller, R. B. Wehrspohn, U. Gosele, and V. Sandoghdar, Phys. Rev. Lett. **58** (2004).
[26] E. Moreno, F. J. Garcia-Vidal, and L. Martin-Moreno, Phys. Rev. B **69** (2004).
[27] W. R. Frei, D. A. Tortorelli, and H. T. Johnson, Opt. Lett. **32**, 77 (2007).
[28] A. Taflove and S. Hagness, *Computational Electrodynamics: The Finite Difference Time-Domain Method* (Artech House, Boston, 2005), p. 285.
[29] Y. K. Lize, E. C. Magi, V. G. Taeed, J. A. Bolger, P. Steinvurzel, and B. J. Eggleton, Opt. Express **12**, 3209 (2004).
[30] H. Nguyen, B. Kuhlmey, M. Steel, C. Smith, E. Mägi, R. McPhedran, and B. Eggleton, Opt. Lett. **30**, 1123 (2005).